Validation of percutaneous puncture trajectory during renal access using 4D ultrasound reconstruction

Pedro L. Rodrigues*[a,b,c], Nuno F. Rodrigues[b,c], Jaime C. Fonseca[b], João L. Vilaça[a,c]
[a]ICVS/3B's - PT Government Associate Laboratory, Braga/Guimarães, Portugal; [b]Algoritmi Center, School of Engineering, University of Minho, Guimarães, Portugal; [c]DIGARC – Polytechnic Institute of Cávado and Ave, Barcelos, Portugal

ABSTRACT

Background: An accurate percutaneous puncture is essential for disintegration and removal of renal stones. Although this procedure has proven to be safe, some organs surrounding the renal target might be accidentally perforated. This work describes a new intraoperative framework where tracked surgical tools are superimposed within 4D ultrasound imaging for security assessment of the percutaneous puncture trajectory (PPT).

Methods: A PPT is first generated from the skin puncture site towards an anatomical target, using the information retrieved by electromagnetic motion tracking sensors coupled to surgical tools. Then, 2D ultrasound images acquired with a tracked probe are used to reconstruct a 4D ultrasound around the PPT under GPU processing. Volume hole-filling was performed in different processing time intervals by a tri-linear interpolation method. At spaced time intervals, the volume of the anatomical structures was segmented to ascertain if any vital structure is in between PPT and might compromise the surgical success. To enhance the volume visualization of the reconstructed structures, different render transfer functions were used.

Results: Real-time US volume reconstruction and rendering with more than 25 frames/s was only possible when rendering only three orthogonal slice views. When using the whole reconstructed volume one achieved 8-15 frames/s. 3 frames/s were reached when one introduce the segmentation and detection if some structure intersected the PPT.

Conclusions: The proposed framework creates a virtual and intuitive platform that can be used to identify and validate a PPT to safely and accurately perform the puncture in percutaneous nephrolithotomy.

Keywords: guided surgery, percutaneous puncture, minimal invasive surgery, electromagnetic tracking sensors, ultrasound reconstruction

1. INTRODUCTION

The prevalence of kidney stones has risen over the past 30 years [1-3]. Nowadays, percutaneous nephrolithotomy (PCNL) is golden standard for treating upper urinary tract stones. The stone clearance rate and treatment outcome is highly dependent on the accuracy of needle puncture in the desired calix [4, 5].

Multiple paths and technological advances have been proposed in the field of urology and minimal invasive surgery to improve this procedure. In what concerns PCNL puncture in particular, the most relevant contributions have been provided by the application of medical imaging techniques, as well as the fusion of multiple imaging procedures [6-9]. Aside from medical imaging, robotic systems [9-11], navigation systems [12-14], finite element models [15, 16] and recent developments in computer graphics and image processing [9], have been proposed in recent years to improve percutaneous puncture.

Despite all the different technological improvements, PCNL puncture step still remains the most challenging task, promoting anatomical targeting errors and damage of vital structures. Although this procedure has proven to be safe, some organs surrounding the renal target might be accidentally perforated. Injuries to the lung, liver, spleen, biliary system, colon, or small bowel have been reported [17, 18].

To this extent, in clinical routine, the PCNL needle puncture is often performed under image guidance [19]. Although medical imaging can provide further information for diagnostic and per-operative planning, it presents some drawbacks.

Medical Imaging 2015: Image-Guided Procedures, Robotic Interventions, and Modeling,
edited by Ziv R. Yaniv, Robert J. Webster III, Proc. of SPIE Vol. 9415, 94152D
 · doi: 10.1117/12.2082528

Real-time images from computed tomography (CT) and fluoroscopy C-arm lead to a significant increase in radiation exposure both to patient and surgeon. On its turn, ultrasounds (US) and magnetic resonance (MR) have proven to be an advantageous imaging option by providing radiation-free real-time imaging. However, their targeting ability for small calculi is limited [7, 20].

In order to reduce imaging dependences, the authors have already tested and evaluated, in animal model, a new real-time electromagnetic tracking (EMT) navigation system for in vivo kidney puncture. Within this previous work, the surgeon performed the percutaneous puncture through a virtual trajectory calculated and displayed in a 3D software [14].

Although capable of directing, correctly and accurately, the puncture path, the previously developed system is unable to guarantee the safeness along the PTT in terms of organs perforation. In order to overcome this drawback, one now presents an evolution of the previous system, resorting to pre-operative US imaging to detect organs in between the PPT and alert for its presence. This system allows the surgeon to: 1) visualize a PPT between the skin puncture site and an anatomical target using an intuitive visual interface; 2) 4D ultrasound imaging around a volume of interest centered in the PPT; and 3) access the security of the PPT.

2. METHODS

2.1 Framework

A Qt/C++ based framework – Renal Puncture (Figure 2) - was developed specially for this work. ITK (Segmentation & Registration Toolkit) libraries were used to aid 4D volume reconstruction and image segmentation. VTK (The Visualization Toolkit) libraries were used only for 3D rendering.

The volume was reconstructed using B-mode ultrasound images acquired using a 3.3 MHz convex probe from Vivid 3 Ultrasound System (GE, Medical Systems). All processing was performed using an Intel Core i7-3770K @ 3.50GHz, NVIDIA GeForce GTX 670 and 16 GB Ram.

The commercially available Aurora electromagnetic tracking system (Northern Digital Inc., Waterloo, Canada) was used to track the catheter tip, needle tip and ultrasound probe during in vitro experiments. The navigation system was composed by (1) one planar low-intensity and varying electromagnetic field generator that establishes a tracking volume; (2) three Aurora sensor interfaces that decrease the possibility of electromagnetic interferences in the testing room; and (3) one 18G/180 mm Chiba needle with 5 degrees of freedom and two ureteral catheter with 1.1 mm diameter and 2 m length with 6 degrees of freedom.

An abdominal ultrasound phantom was used to test this new methodology. It includes all abdominal organs (spleen, liver, colon and the urinary collecting system) that might be injured during renal access.

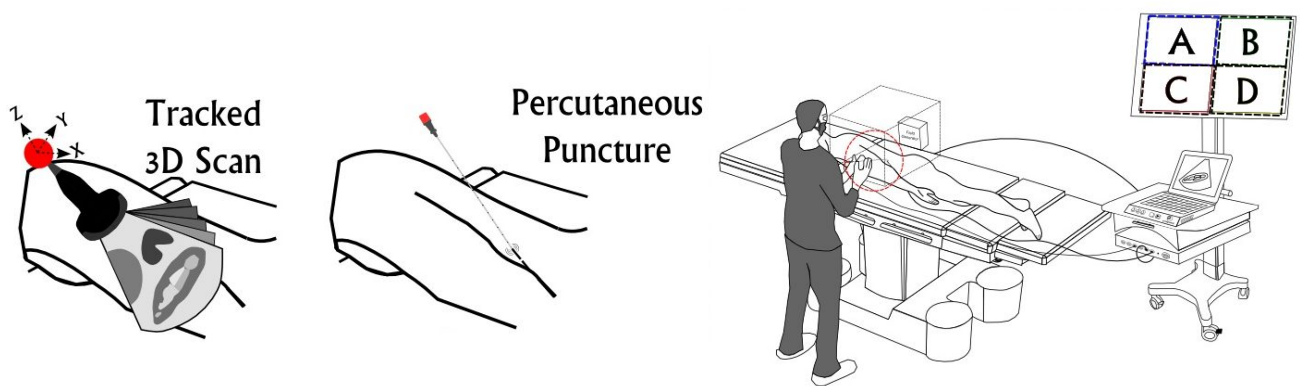

Figure 1. Overview of the 4D freehand ultrasound for PPT security validation: (left) ultrasound scan along the PPT using a tracked probe; (center) percutaneous puncture using a catheter and needle that integrate electromagnetic sensors; (right) possible surgical setup comprising the Aurora field generator, tracking volume around the patient abdominal area, ultrasound machine and interface monitor for percutaneous guidance.

2.2 System overview

A system overview is shown in Figure 1.

At the first surgical step, a catheter will be inserted and guided, through an ureterorenoscope with a camera and guided tip, trans-urethrally towards the renal calix. This catheter will have a position and orientation electromagnetic sensor on its tip that will function as a real-time anatomic target locator. At the next step, the puncture one, it will be used a needle that also integrates a similar sensor. From the data provided by both sensors, it will be possible to define the PPT from where the needle will be inserted [14, 21].

This PPT will be presented to the surgeon using a graphical user interface. Here, the surgeon will be guided in order to create an ultrasound reconstructed volume using a tracked probe in order to evaluate the risk of possible perforation of vital anatomic structures. When, the PPT is checked and approved by the surgeon, the puncture procedure will be conducted without further imaging modalities. The puncture success is assured using the ureterorenoscope video camera.

2.3 4D ultrasound reconstruction

To provide PPT intraoperative imaging during percutaneous nephrolithotomy, the presented framework can reconstruct 3D and 4D ultrasound by freehand scanning using a tracked convex ultrasound probe.

2D US images, acquired with a tracked probe, were used to reconstruct a 4D ultrasound around the PPT. This volume was used to ascertain that any vital structure is in between both sensors and might compromise the surgical success.

Before testing, an Aurora catheter sensor was mounted on the ultrasound probe and calibrated using Strdx software [22]. It integrates automatic spatial and temporal calibration systems for 3D ultrasound. Firstly, a fabricated non-ferromagnetic mold rigidly attaches the sensor on the body of the ultrasound probe. Then, a 30x30x15 cm box filled with distilled water at room temperature and a flat and roughen bottom (made of cork), was used to improve the reflection of ultrasound at oblique angles. The calibration process was performed by moving the probe while imaging the bottom of the water bath by: (1) moving the probe vertically up and down without changing its orientation; (2) rotating the probe in each 3D coordinate axis (each axis individually and then all together) while keeping the scan plane and the phantom plane perpendicular; (3) translate the probe while performing motions (1) and (2). Simultaneously, Stradx track the bottom of the water bath in the image with a line detector algorithm [22]. By matching the image motion and the Aurora tracking readings, it was possible to estimate a temporal calibration the position and image streams.

After de calibration, real-time ultrasound reconstruction was achieved using different synchronized and parallel threads:

(1) Thread one buffers and receives ultrasound frames: each video frame was resampled by a factor of 2 and allocated onto an image stack along with a timestamp tv that describes when the video was acquired. The video was captured at full rate of 30 frames/s;

(2) Thread two receives and processes tracking data: the Aurora tracking information, received via serial port, was converted to a 4 by 4 matrix and pre-allocated along with a timestamp tA that describes when the tracking data was acquired;

(3) Thread three triggers a signal that specifies the starting of a new cardiac cycle for reconstruction gating. Since kidney and surround tissues may move during the reconstruction process, they must be inserted into the partially 3D volume at similar points of the cardiac cycle. To this extent, the user must specified an expected heart rate for the reconstruction procedure by averaging the heart rates recorded over a user-specified time period;

(4) Thread four updates the partially reconstructed volume, under GPU processing, by inserting the most recent US frame. Every time that Thread three triggers a signal, the period of the previous cycle is used to predict the timestamps for the upcoming cycle. The ultrasound frames and tracking matrices, with timestamps tv and tA, that are closest to these predicted values are inserted into the correct output volume using the associated tracking transforms;

(5) Thread five processes volume rendering of the output volume using color and opacity transfer functions (Figure 1-C);

(6) Thread six displays the partially reconstructed 3D ultrasound volume into the main application;

(7) Thread seven assures that there are no gaps in the reconstructed volume by triggering a function every 200 ms that searches all empty voxels and modifies its voxel intensity using a tri-linear interpolation method of the closest non-empty voxels.

2.4 PPT security assessment

Thread eight assured multi-organ segmentation of volume structures and its intersection with the PPT. For segmentation, the image histogram was smoothed by solving a non-linear diffusion equation [23]. The Tukey's biweight as edge-stopping diffusivity function (1):

$$g(x,\sigma)=\begin{cases}1/2\left[1-(x/\sigma)^2\right]^2, |x|\leq\sigma \\ 0, |x|\leq\sigma\end{cases} \tag{1}$$

was used to create a more accurate histogram underlying different groups of objects. By estimating the histogram local maximums (specified histogram region that is concave down) it was possible to define multi-threshold levels that create 8-connected labels of different structures.

The kidney label was automatically identified by choosing the most cylindrical and largest structure in a 5 cm radius (approximately the kidney size) around the Aurora catheter sensor (real-time anatomic target locator). Then, the points along the PPT were intersected with image labelled regions. When the user starts the puncture procedure, the framework will assume that all structures that intersects the PPT are not vital and can be perforated. From there, if any anatomical structure changes along the PPT, the framework will advise the user by rendering a text and sound alert. Here, the surgeon must accept or reject this new structure as a possible vital structure and continues the puncture procedure.

3. RESULTS

The calibration process was performed only one time before US reconstruction and took about 6 minutes. Any further calibration was not necessary as long as the Aurora sensor does not change its position relative to ultrasound probe body. A slight latency of around 16 ms between the tracking system and ultrasound video was accurately measured with Stradx software [24] and accurately compensated during reconstruction.

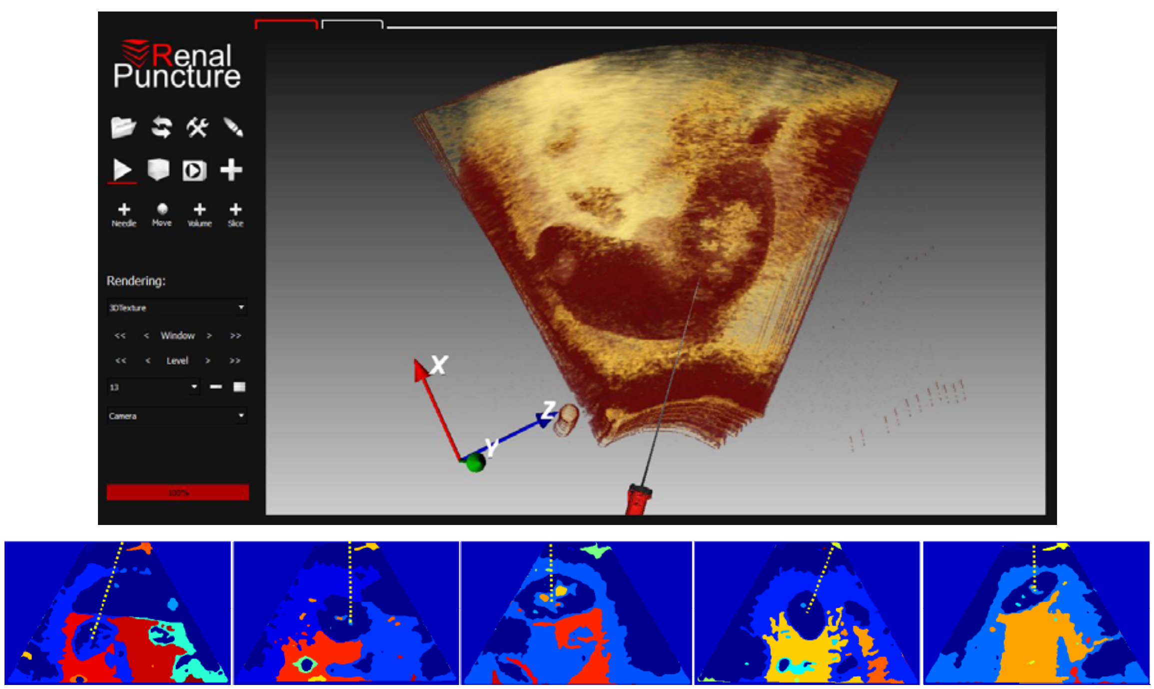

Figure 2. (up) Overview of the Renal puncture Framework; (down) Segmentation results with random PPT (yellow).

Thirty-seven US phantom volumes were reconstructed with different probe orientations. Real-time US volume reconstruction and rendering with more than 25 frames/s was only possible when only three orthogonal slice views where rendered to the user. When using the whole reconstructed volume, one achieved 15 frames/s for volume with size 7x7x15 cm3 and 8 frames/s for 10x10x15 cm3. When labelling the different image structures we obtained 3 frames/s.

The segmentation process were able to identify if any anatomical structure was in between the PPT with an efficiency of 98.89±4.28% along the PPT. The median time for ultrasound checking was 3.5 min (range 2-6 min) while the puncture step was performed in 25 seconds (range 15-54s) for doctors.

4. DISCUSSION

Although 4D ultrasound visualization has been integrated into commercial ultrasound systems [25], the inaccessibility of raw image data makes these system unsuitable for personalized guided surgery, advanced visualization and virtual navigation. A significant advantage of the Renal Puncture framework over literature is that both 3D and 4D ultrasound can be generated in real-time and, at the same time, different volume structures are segmented and evaluated if they intersect the PPT. The proposed framework creates a virtual and intuitive platform that can be used to identify and validate a PPT to safely and accurately perform the puncture during percutaneous nephrolithotomy.

Comparing to state of the art results, the need for image registration with pre-operative imaging was eliminated by using ultrasound checking and a miniaturized sensor that can be inserted near the anatomical target [13]. The uncertainty of possible anatomical structures in between puncture path [14, 21] was reduced by performing a 4D ultrasound before the puncture step around the puncture site. Although, compared with the work described by the authors in [14], the time for puncture planning increases with a median of 3.5 minutes, the uncertainty of some anatomical structure in between the PPT is eliminated.

Since medical imaging assistance to puncture commonly requires approximately 10 min [26-29], the puncture step itself remains faster than any literature approach, without any radiation exposure.

Although some motion artifacts where presented in the 4D ultrasound reconstruction, they did not interfere with the puncture path security assessment. Further wok needs to be conducted in particular considering *in vivo* testing. On the other hand, since minimally invasive surgical procedures comprising percutaneous puncture of the kidney are highly dependent on the accuracy that the needle reaches the desired target, further work may also include an automatic and real time kidney segmentation.

5. CONCLUSION

This paper describes a new intuitive framework for security assessment of PPT for renal access guided using EMT sensors. This new approach can guarantee the safeness of the percutaneous puncture trajectory in terms of organs perforation for the system already proposed by the authors [14].

The synergy of ultrasound checking and tracking modalities will allow puncture guidance through the optimal path towards the precise calculus location. This framework may increase surgeon's confidence and reduce possible complications such as organ perforation. In addition, it has the potential to make percutaneous renal access free of ionizing radiation for both patient and surgeon.

ACKNOWLEDGMENT

The authors acknowledge to Foundation for Science and Technology (FCT) - Portugal for the fellowships with references: SFRH/BD/74276/2010. The present submission corresponds to original research work of the authors and has never been submitted elsewhere for publication.

REFERENCES

[1] C. M. Cracco, C. M. Scoffone, and R. M. Scarpa, “New developments in percutaneous techniques for simple and complex branched renal stones,” Curr Opin Urol, (2011).

[2] A. Skolarikos, G. Alivizatos, and J. J. M. C. H. de la Rosette, “Percutaneous nephrolithotomy and its legacy,” European Urology, 47(1), 22-28 (2005).

[3] E. M. Worcester, and F. L. Coe, “Calcium Kidney Stones,” New England Journal of Medicine, 363(10), 954-963 (2010).

[4] J. W. Pugh, and B. K. Canales, “New instrumentation in percutaneous nephrolithotomy,” Indian J Urol, 26(3), 389-94 (2010).

[5] R. Viard, N. Betrouni, J. Rousseau et al., “Needle positioning in interventional MRI procedure: real time optical localisation and accordance with the roadmap,” Conf Proc IEEE Eng Med Biol Soc, 2007, 2748-51 (2007).

[6] Z. C. Li, K. Li, H. L. Zhan et al., “Augmenting intraoperative ultrasound with preoperative magnetic resonance planning models for percutaneous renal access,” Biomed Eng Online, 11, 60 (2012).

[7] C. Kalogeropoulou, P. Kallidonis, and E. N. Liatsikos, “Imaging in Percutaneous Nephrolithotomy,” Journal of Endourology, 23(10), 1571-1577 (2009).

[8] M. J. Bader, C. Gratzke, M. Seitz et al., “The "All-Seeing Needle": Initial Results of an Optical Puncture System Confirming Access in Percutaneous Nephrolithotomy,” European Urology, 59(6), 1054-1059 (2011).

[9] O. Ukimura, “Image-guided surgery in minimally invasive urology,” Current Opinion in Urology, 20(2), 136-140 10.1097/MOU.0b013e3283362610 (2010).

[10] M. M. Desai, R. Grover, M. Aron et al., “Robotic Flexible Ureteroscopy for Renal Calculi: Initial Clinical Experience,” Journal of Urology, 186(2), 563-568 (2011).

[11] P. Mozer, J. Troccaz, and D. Stoianovici, “Urologic robots and future directions,” Current Opinion in Urology, 19(1), 114-119 (2009).

[12] Z. Yaniv, E. Wilson, D. Lindisch et al., “Electromagnetic tracking in the clinical environment,” Medical Physics, 36(3), 876-892 (2009).

[13] P. L. Rodrigues, A. H. J. Moreira, N. F. Rodrigues et al., "Preliminary clinical trial in percutaneous nephrolithotomy using a real-time navigation system for percutaneous kidney access." 9036, 903606-903606-7.

[14] P. L. Rodrigues, J. L. Vilaça, C. Oliveira et al., “Collecting system percutaneous access using real-time tracking sensors: First pig model in vivo experience,” The Journal of urology, 190(5), 1932-1937 (2013).

[15] J. T. Hing, A. D. Brooks, and J. P. Desai, “A biplanar fluoroscopic approach for the measurement, modeling, and simulation of needle and soft-tissue interaction,” Medical Image Analysis, 11(1), 62-78 (2007).

[16] D. J. van Gerwen, J. Dankelman, and J. J. van den Dobbelsteen, “Needle-tissue interaction forces - A survey of experimental data,” Medical Engineering & Physics, 34(6), 665-680 (2012).

[17] J. d. l. Rosette, D. Assimos, M. Desai et al., “The clinical research office of the endourological society percutaneous nephrolithotomy global study: indications, complications, and outcomes in 5803 patients,” Journal of endourology, 25(1), 11-17 (2011).

[18] P. D. Voilette, and J. D. Denstedt, “Standardizing the reporting of percutaneous nephrolithotomy complications,” Indian journal of urology: IJU: journal of the Urological Society of India, 30(1), 84 (2014).

[19] P. L. Rodrigues, N. F. Rodrigues, J. Fonseca et al., “Kidney Targeting and Puncturing During Percutaneous Nephrolithotomy: Recent Advances and Future Perspectives,” Journal of Endourology, 27(7), 826-834 (2013).

[20] H. Karami, A. H. Arbab, A. Rezaei et al., “Percutaneous nephrolithotomy with ultrasonography-guided renal access in the lateral decubitus flank position,” Journal of Endourology, 23(1), 33-5 (2009).

[21] J. Huber, I. Wegner, H. P. Meinzer et al., "Navigated renal access using electromagnetic tracking: an initial experience," Surgical Endoscopy and Other Interventional Techniques, 25(4), 1307-1312 (2011).

[22] L. Barber, R. Barrett, and G. Lichtwark, "Validation of a freehand 3D ultrasound system for morphological measures of the medial gastrocnemius muscle," Journal of biomechanics, 42(9), 1313-1319 (2009).

[23] J. Weickert, and H. Scharr, "A scheme for coherence-enhancing diffusion filtering with optimized rotation invariance," Journal of Visual Communication and Image Representation, 13(1), 103-118 (2002).

[24] R. W. Prager, A. Gee, and L. Berman, "Stradx: real-time acquisition and visualization of freehand three-dimensional ultrasound," Medical Image Analysis, 3(2), 129-140 (1999).

[25] O. V. Solberg, F. Lindseth, H. Torp et al., "Freehand 3D ultrasound reconstruction algorithms—a review," Ultrasound in medicine & biology, 33(7), 991-1009 (2007).

[26] X. Li, S. Liao, Y. Yu et al., "Stereotactic localisation system: a modified puncture technique for percutaneous nephrolithotomy," Urological Research, 40(4), 395-401 (2012).

[27] H. Karami, R. Mohammadi, and B. Lotfi, "A study on comparative outcomes of percutaneous nephrolithotomy in prone, supine, and flank positions," World Journal of Urology, 1-6 (2012).

[28] M. Ritter, M. C. Rassweiler, A. Häcker et al., "Laser-guided percutaneous kidney access with the Uro Dyna-CT: first experience of three-dimensional puncture planning with an ex vivo model," World Journal of Urology, 1-5 (2012).

[29] O. Tanriverdi, U. Boylu, M. Kendirci et al., "The learning curve in the training of percutaneous nephrolithotomy," European Urology, 52(1), 206-212 (2007).